Pressure Perturbation and Differential Scanning Calorimetric Studies of Bipolar Tetraether Liposomes Derived from the Thermoacidophilic Archaeon *Sulfolobus acidocaldarius*

Parkson Lee-Gau Chong,* Revanur Ravindra,† Monika Khurana,† Verrica English,* and Roland Winter†
*Department of Biochemistry, Temple University School of Medicine, Philadelphia, Pennsylvania; and †Department of Chemistry, Physical Chemistry I, University of Dortmund, Dortmund, Germany

ABSTRACT Differential scanning calorimetry (DSC) and pressure perturbation calorimetry (PPC) were used to characterize thermal phase transitions, membrane packing, and volumetric properties in multilamellar vesicles (MLVs) composed of the polar lipid fraction E (PLFE) isolated from the thermoacidophilic archaeon *Sulfolobus acidocaldarius* grown at different temperatures. For PLFE MLVs derived from cells grown at 78°C, the first DSC heating scan exhibits an endothermic transition at 46.7°C, a small hump near 60°C, and a broad exothermic transition at 78.5°C, whereas the PPC scan reveals two transitions at ~45°C and 60°C. The endothermic peak at 46.7°C is attributed to a lamellar-to-lamellar phase transition and has an unusually low ΔH (3.5 kJ/mol) and $\Delta V/V$ (0.1%) value, as compared to those for the main phase transitions of saturated diacyl monopolar diester lipids. This result may arise from the restricted *trans-gauche* conformational changes in the dibiphytanyl chain due to the presence of cyclopentane rings and branched methyl groups and due to the spanning of the lipid molecules over the whole membrane. The exothermic peak at 78.5°C probably corresponds to a lamellar-to-cubic phase transition and exhibits a large and negative ΔH value (–23.2 kJ/mol), which is uncommon for normal lamellar-to-cubic phospholipid phase transformations. This exothermic transition disappears in the subsequent heating scans and thus may involve a metastable phase, which is irreversible at the scan rate used. Further, there is no distinct peak in the plot of the thermal expansion coefficient α versus temperature near 78.5°C, indicating that this lamellar-to-cubic phase transition is not accompanied by any significant volume change. For PLFE MLVs derived from cells grown at 65°C, similar DSC and PPC profiles and thermal history responses were obtained. However, the lower growth temperature yields a higher $\Delta V/V$ (~0.25%) and ΔH (14 kJ/mol) value for the lamellar-to-lamellar phase transition measured at the same pH (2.1). A lower growth temperature also generates a less negative temperature dependence of α. The changes in $\Delta V/V$, ΔH, and the temperature dependence of α can be attributed to the decrease in the number of cyclopentane rings in PLFE at the lower growth temperature. The relatively low $\Delta V/V$ and small ΔH involved in the phase transitions help to explain why PLFE liposomes are remarkably thermally stable and also echo the proposal that PLFE liposomes are generally rigid and tightly packed. These results help us to understand why, despite the occurrence of thermal-induced phase transitions, PLFE liposomes exhibit a remarkably low temperature sensitivity of proton permeation and dye leakage.

INTRODUCTION

Of the lipid components of the plasma membrane of the thermoacidophilic archaeon *Sulfolobus Acidocaldarius*, ~90% are dibiphytanyldiglycerol tetraether lipids (1,2), among which the polar lipid fraction E (PLFE) is one of the main constituents (3). PLFE contains a mixture of bipolar tetraether lipids with either a glycerol dialkylcalditol tetraether (GDNT or calditoglycerocaldarchaeol) or a glycerol dialkylglycerol tetraether (GDGT, or caldarchaeol) skeleton (3–5). GDNT (~90% of total PLFE) contains phosphomyoinositol on the glycerol end and β-glucose on the calditol end, whereas GDGT (~10% of total PLFE) has phosphomyoinositol attached to one glycerol and β-D-galactosyl-D-glucose attached to the other glycerol skeleton. Both GDGT and GDNT are bisubstituted in the polar headgroup regions, thus designated as bipolar tetraether lipids. The nonpolar regions of these lipids consist of a pair of 40-carbon biphytanyl chains, each of which contains up to four cyclopentane rings. The number of the cyclopentane rings in each biphytanyl chain increases with increasing growth temperature (6).

PLFE lipids form stable multilamellar vesicles (MLV) and unilamellar liposomes in aqueous solutions by shaking and extrusion, respectively (3). PLFE lipids can also form stable giant unilamellar vesicles (~20–150 μm in diameter) by the electroformation method (7). In PLFE liposomes, lipids span the entire lamellar structure, forming a monomolecular thick membrane (8), in contrast to the bilayer structure formed by monopolar diester (or diether) phospholipids. Since PLFE is a major polar lipid component in the plasma membrane of *S. acidocaldarius*, PLFE liposomes have been used as a model system for studying thermoacidophilic archaeal membranes.

PLFE liposomes exhibit high thermal stability and unusually low solute permeability when compared to monopolar

Submitted April 1, 2005, and accepted for publication June 17, 2005.

Address reprint requests to Dr. Roland Winter, Dept. of Chemistry, University of Dortmund, Otto-Hahn-Strasse 6, D-44227, Dortmund, Germany. Tel.: 49-231-755-3900; Fax: 49-231-755-3901; E-mail: winter@pci.chemie.uni-dortmund.de; or to Dr. Parkson Chong, Dept. of Biochemistry, Temple University School of Medicine, Philadelphia, PA 19140. Tel.: 215-707-4182; Fax: 215-707-7536; E-mail: pchong02@temple.edu.

0006-3495/05/09/1841/09 $2.00

doi: 10.1529/biophysj.105.063933

diester or diether liposomes (reviewed in Gliozzi et al. (5)). The thermal stability with respect to leakage of dye originally trapped inside PLFE liposomes has been attributed to the negative charges on the membrane surface and to the tight and rigid lipid packing (9–11). The low proton permeability in PLFE liposomes has been ascribed to the network of hydrogen bonds between the sugar residues of PLFE exposed at the outer face of the membrane (10) and to the tight and rigid lipid packing (11,12). Both the dye leakage and proton permeation experiments suggest that membrane packing, in either the hydrocarbon or the polar headgroup regions or both, is a central issue in understanding PLFE lipid membranes.

To study membrane packing in PLFE liposomes, lateral and rotational diffusions of membrane probes have been examined. The lateral mobility of 1-palmitoyl-2-(10-pyrenyl)-decanoyl)-*sn*-glycero-3-phosphatidylcholine (PyrPC) in PLFE liposomes was found to be highly restricted and only became appreciable at temperatures >48°C (13), a result confirmed later by a ^{31}P-NMR study on similar tetraether liposomes (14). Using a multiexcitation method, we also detected an abrupt increase in the rotational rates of perylene in PLFE liposomes at ~48°C (15). These results indicate a significant structural change near 48°C in the PLFE hydrocarbon core, where the chromophores of perylene and PyrPC are supposed to reside. These studies also suggest that the hydrocarbon region of PLFE liposomes is rigid and tightly packed below ~48°C. Above ~48°C, the hydrocarbon core of PLFE membranes begins to gain appreciable membrane fluidity, which would be required for the functionality of archaeal membranes.

The polar headgroup region of PLFE membranes, on the other hand, may still be rigid and tightly packed through the hydrogen-bond network (16,17) at elevated temperatures (>48°C) so as to maintain a large proton gradient (pH 2–3 outside and pH 6.5 inside the cell) across the membrane at the growth temperature. This proposition explains why low proton permeability and appreciable membrane fluidity can occur at the same time in thermoacidophiles at high growth temperatures. This point is supported by a spin-label study, which showed that at high temperatures (~85°C) the nonitol (more precisely, calditol) headgroup of tetraether lipids from the thermoacidophilic archaeon *Sulfolobus solfataricus* was relatively immobile and that the rotation of the spin-label probe was still anisotropic, whereas the hydrocarbon region possessed some mobility (18).

In this study, pressure perturbation calorimetry (PPC) was used to further characterize membrane packing and phase behaviors of PLFE liposomes. PPC allowed for the determination of the thermal volume expansion coefficient, α, as a function of temperature. From the plot of α versus T, the phase transitions that involve significant volume changes were detected and the relative volume changes ($\Delta V/V$) associated with the phase transitions were calculated. In addition to PPC, differential scanning calorimetry (DSC) was employed to detect the phase transitions involving significant enthalpy changes (ΔH). $\Delta V/V$, ΔH, and the temperature dependence of α for PLFE MLVs derived from two different cell growth temperatures, i.e., 65 and 78°C, were compared.

MATERIALS AND METHODS

Materials

S. acidocaldarius cells (ATCC 49426, Rockville, MD) were grown aerobically and heterotrophically at 65 or 78°C and at pH 2.5–3.0. The growth was monitored by absorbance at 420 and 540 nm. The cells were harvested just before the stationary phase. PLFE lipids were isolated from *S. acidocaldarius* dry cells as previously described (3,19). Dipalmitoyl-L-α-phosphatidylcholine (DPPC) was purchased from Avanti Polar Lipids (Alabaster, AL).

Preparation of PLFE liposomes

PLFE liposomes were prepared by dissolving PLFE lipids in chloroform/methanol/water (65:25:10, v/v/v), vortex-mixing the solution in sealed containers and drying the solution first under a stream of nitrogen gas and then under vacuum for at least 16 h. The dried lipid was dispersed in D_2O or citrate buffer/H_2O and the pH was adjusted to the desired value. Measurements in D_2O as solvent were carried out to compare the data with literature results from Fourier transform infrared spectroscopic and small-angle x-ray scattering data. The hydrated mixture was heated in a closed vessel to a temperature of 70°C and vortex-mixed for at least 5 min to yield MLVs. MLVs were subjected to five to six freeze-thaw cycles before DSC or PPC measurements.

Differential scanning calorimetry

DSC measurements were made with a VP DSC calorimeter from MicroCal (Northampton, MA). The sample cell of the calorimeter was filled with ~0.5 mL of solution, with a concentration of 5 mg/mL, whereas the reference cell was filled with a matching aqueous solution. Both heating and cooling scans were made at a scan rate of 20°C/h. Before each heating scan, the vesicles were kept at starting temperature for ~2 h. C_p values are given with respect to the reference cell.

Pressure perturbation calorimetry

PPC measurements were performed on the same MicroCal calorimeter equipped with a MicroCal pressurizing cap. A nitrogen gas pressure of ~5 bar was applied to the samples (5 mg/mL) during all PPC cycles (20,21). The effective scan rate was 20°C/h. Under the same experimental conditions, a set of reference sample-water and water-water measurements was carried out each time. For calculation of the relative volume changes, a partial specific lipid volume of 1 $cm^3\ g^{-1}$ was used.

RESULTS AND DISCUSSION

DSC thermograms measured at pH 2.1 for PLFE MLVs derived from cells grown at 78°C

Fig. 1 shows three consecutive heating DSC scans of MLVs composed of PLFE lipids isolated from *S. acidocaldarius* grown at 78°C. The sample was measured in D_2O at pH 2.1. The first scan displays an endothermic peak at 46.7°C

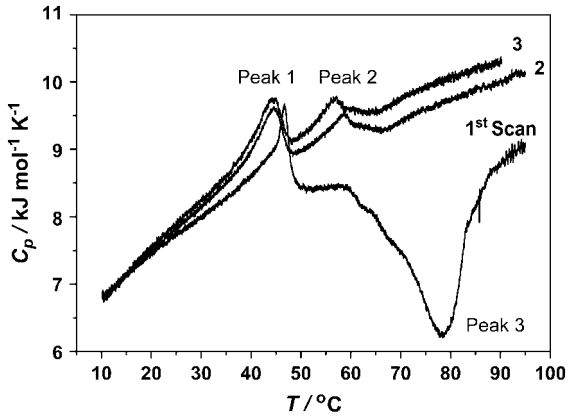

FIGURE 1 DSC thermograms, measured at pH 2.1, of PLFE MLVs derived from cells grown at 78°C. All the scans presented in this study were obtained in the heating mode.

(*Peak 1* in Scan 1), a small hump near 60°C (*Peak 2* in Scan 1), and a broad exothermic transition centered at 78.5°C (*Peak 3* in Scan 1). The peak at 46.7°C (*Peak 1*) is in good agreement with the lamellar-to-lamellar phase transition previously observed at ~50°C by small-angle x-ray scattering (22), ~46–48°C by infrared (22), ~48°C by perylene rotational rate (15), ~48°C by PyrPC excimer fluorescence (13), and ~50°C by generalized polarization of Laurdan (2-dimethylamino-6-lauroyl-naphthalene) fluorescence (7). The transition temperature of Peak 1 changes little (from 47 to 45°C) in three consecutive heating scans (Fig. 1).

The broad exothermic transition at 78.5°C in Scan 1 (Fig. 1) corresponds to the phase transition from lamellar to probably inverted bicontinuous cubic phases (Q_{II}^D and Q_{II}^P) previously detected at ~74–75°C by small-angle x-ray scattering (22). The broadness of this transition may be attributed to the coexistence of Q_{II}^D and Q_{II}^P, and the chemical heterogeneity of PLFE. If there is a transition from a lamellar to two cubic phases, there exists a broad phase coexistence region, which smears out the transition. The assignment to the coexistence of Q_{II}^D and Q_{II}^P phases is based on the small-angle x-ray diffraction pattern and the calculated ratio of the lattice constants of the cubic structures Q_{II}^D and Q_{II}^P, as explained in Chong et al. (22). The exothermic transition, however, disappears in the second and third heating scans (Fig. 1), suggesting that the thermal-induced phase transition at ~78.5°C involves a metastable phase, which is irreversible at the scan rate used (20°C/h). Metastable phases with rather long restoration times have in fact been observed in many lipid systems (23,24), including phospholipid systems involving inverted cubic phases (25–27). Liposomes made of total lipid extracts from a similar thermoacidophilic archaeon, *S. solfataricus*, also exhibited evidence for cubic phase formation at high temperatures (28–30). The small hump near 60°C in Scan 1 turns out to be a distinct endothermic peak at 57–59°C in Scan 2 and Scan 3 (*Peak 2* in Fig. 1). This phase transition corresponds to the lamellar-to-lamellar phase transition at ~60–61°C previously detected by infrared and small-angle x-ray scattering (22). Thus, all the DSC peaks shown in Fig. 1 can be attributed to the phase transitions of PLFE liposomes previously detected by other techniques, and the three consecutive heating scans (Fig. 1) reveal how those phase transitions vary with sample thermal history.

In addition to the transition temperature (T_{tr}), the DSC thermograms (Fig. 1) allow us to determine the transition temperature span ($T_{1/2}$) and the enthalpy change (ΔH) of the phase transitions (Table 1). The ΔH value of Peak 1 in all three heating scans obtained from PLFE MLVs (Table 1) is ~7, 10, or 13 times smaller than that for the main phase transition of MLVs composed of dimyristoyl-L-α-phosphatidylcholine (DMPC) (31), DPPC (32), or distearoyl-L-α-phosphatidylcholine (DSPC) (32), respectively. The ΔH value of Peak 1 from PLFE MLVs is similar to that for the

TABLE 1 DSC and PPC parameters of PLFE liposomes derived from cells grown at 78°C, pH 2.1

	Peak 1			Peak 2			Peak 3		
DSC	T_{tr} (°C)	ΔH (kJ/mol)	$T_{1/2}$ (°C)	T_{tr} (°C)	ΔH (kJ/mol)	$T_{1/2}$ (°C)	T_{tr} (°C)	ΔH (kJ/mol)	$T_{1/2}$ (°C)
Scan 1	46.7	3.5	1.9	N.D.	N.D.	N.D.	78.5	–23.2	10.0
Scan 2	44.6	4.2	4.7	58.6	2.0	3.7	N.D.	N.D.	N.D.
Scan 3	44.2	3.7	4.9	57.1	1.5	3.0	N.D.	N.D.	N.D.
	T_{tr} (°C)	ΔH (J/g)	$T_{1/2}$ (°C)	T_{tr} (°C)	ΔH (J/g)	$T_{1/2}$ (°C)	T_{tr} (°C)	ΔH (J/g)	$T_{1/2}$ (°C)
Scan 1	46.7	1.5	1.9	N.D.	N.D.	N.D.	78.5	–10.1	10.0
Scan 2	44.6	1.8	4.7	58.6	0.9	3.7	N.D.	N.D.	N.D.
Scan 3	44.2	1.6	4.9	57.1	0.7	3.0	N.D.	N.D.	N.D.
	Peak 1			Peak 2			Peak 3		
PPC	T_{tr} (°C)	$\Delta V/V$ (%)	$T_{1/2}$ (°C)	T_{tr} (°C)	$\Delta V/V$ (%)	$T_{1/2}$ (°C)	T_{tr} (°C)	$\Delta V/V$ (%)	$T_{1/2}$ (°C)
Scan 1	45	0.10	3.7	60.0	0.09	4.5	N.D.	N.D.	N.D.
Scan 2	43	0.14	4.5	57.5	0.08	4.5	N.D.	N.D.	N.D.

The molar ΔH, in terms of kJ/mol, was calculated based on an estimated molecular mass of 2300 for PLFE. T_{tr}, phase transition temperature; $T_{1/2}$, transition width; ΔH, enthalpy change associated with the phase transition; N.D., not detected.

pretransition in DMPC MLVs, but still approximately two times smaller than the ΔH value of the pretransitions of DPPC MLVs (33). The low ΔH value for PLFE MLVs suggests that the lamellar-to-lamellar phase transition of Peak 1 involves restricted *trans-gauche* conformational changes in the PLFE dibiphytanyl chains due to the presence of the cyclopentane ring, branched methyl groups, and the bipolar nature of the PLFE lipids, and due to the spanning of the dibiphytanyl chains through the membrane. In contrast, the main phase transition of diacylphosphatidylcholines (e.g., DMPC, DPPC, and DSPC) entails extensive *trans-gauche* conformational changes along the polymethylene chains. It is also noticed from Table 1 that Peak 1 in PLFE MLVs is ~20 times broader than the main transition of DMPC MLVs (31). The broadness reflects a rather low cooperativity of the transition, which can be attributed to the fact that PLFE is a mixture of GDNT and GDGT with varying numbers of cyclopentane rings. On the other hand, the transition width of Peak 1 in PLFE MLVs (Table 1) is ~4–10 times narrower than that in equimolar DMPC/DSPC bilayers, which exhibit a rather strong nonideal mixing behavior, suggesting that the coexistence of many different gel and fluid clusters seen in equimolar DMPC/DSPC mixtures (34) is not likely to occur, or occurs to a much lesser extent, during the lamellar-to-lamellar phase transition of PLFE MLVs.

The ΔH (–23.2 kJ/mol) for Peak 3 in Scan 1 is large and negative (exothermic) (Table 1), which is atypical for the fluid lamellar-to-cubic phase transitions found in normal lipid systems. For example, the liquid crystalline-to-cubic phase transition of *N*-methylated dioleoylphosphatidylethanolamine (DOPE-Me) is endothermic, with a transition enthalpy of 0.63 kJ/mol (or 150 cal/mol) (26). Another difference is that the cubic phase of DOPE-Me is reliably detected by calorimetry only when a slow scan rate (~1–2°C/h) is used (26,35), whereas in this study the cubic phase of PLFE MLVs is detectable at a scan rate of 20°C/h and an extensive incubation (18–20 h for DOPE-Me (26)) of the membrane at high temperature is not required. The transition temperature width ($T_{1/2}$) for Peak 3 of Scan 1 (Table 1) is much broader than that for DOPE-Me (26), which again can be attributed to the chemical heterogeneity of PLFE.

DSC thermograms measured at pH 2.1 for PLFE MLVs derived from cells grown at 65°C

Fig. 2 (*bottom curve*) shows that the first DSC heating thermogram (measured at pH 2.1) of PLFE MLVs derived from cells grown at 65°C exhibits one endothermic (at 51°C) and one exothermic (at 83.2°C) transition, similar to the case for cells grown at 78°C (Fig. 2, *top curve*; also Scan 1 in Fig. 1), in terms of the overall profile. The high-temperature exothermic transition in both curves (Fig. 2) may be attributed to the formation of cubic phases. The finding that cubic phases can be formed from PLFE lipids derived from different growth

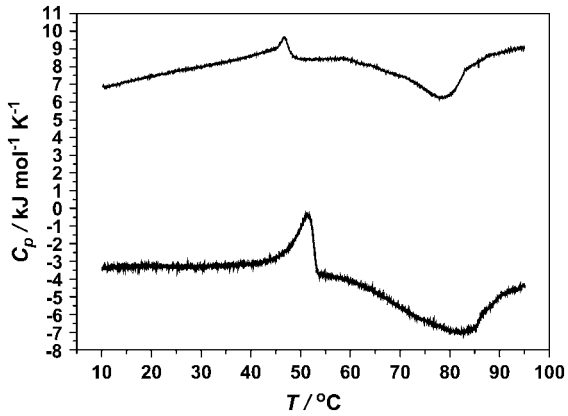

FIGURE 2 Comparison of DSC thermograms, measured at the same pH (2.1), for PLFE MLVs derived from cells grown at 78°C (*top*) and 65°C (*bottom*).

temperatures implies that the number of cyclopentane rings is not critical for the formation of cubic phases, which seem to occur close to or above the growth temperature (Tables 1 and 2).

Table 2 compares the T_{tr}, ΔH, and $T_{1/2}$ values of the two curves shown in Fig. 2. The ΔH value (Table 2) of Peak 1 in PLFE MLVs derived from a growth temperature of 65°C (Fig. 2, *bottom curve*) is ~4 times higher than that in PLFE MLVs derived from a growth temperature of 78°C (Fig. 2, *top curve*). This may result from the decrease in the number of cyclopentane rings in PLFE at the lower cell growth temperature (6). When the number of the cyclopentane rings is decreased, *trans-gauche* conformational changes in the dibiphytanyl chain would be enhanced due to less rotational restriction, resulting in a higher ΔH value. On the other hand, the growth temperature variation, or inferentially the change in the number of PLFE cyclopentane rings, does not seem to greatly affect the ΔH value of the lamellar-to-cubic phase transition (–23.2 kJ/mol vs. −18.0 kJ/mol) (Table 2).

DSC thermograms measured at pH 7.0 for PLFE MLVs derived from cells grown at 65°C

The effect of pH on the DSC thermograms for PLFE MLVs derived from the same growth temperature was also examined.

TABLE 2 Comparison of the T_{tr}, $T_{1/2}$, and ΔH of PLFE liposomes derived from cells grown at different temperatures

	Endothermic peak			Exothermic peak		
	T_{tr} (°C)	ΔH (kJ/mol)	$T_{1/2}$ (°C)	T_{tr} (°C)	ΔH (kJ/mol)	$T_{1/2}$ (°C)
Sample 1 (cells grown at 78°C)	46.7	3.5	1.9	78.5	−23.2	10
Sample 2 (cells grown at 65°C)	51.0	14.2	3.8	83.2	−18.0	14

Data were obtained from the first DSC heating scans (Fig. 2) measured at pH 2.1.

Shown in Fig. 3 are three consecutive DSC heating scans measured at pH 7.0, whereas the bottom curve of Fig. 2 shows the DSC profile measured at pH 2.1, all for PLFE MLVs derived from cells grown at 65°C. The first heating scan in Fig. 3 shows one endothermic peak (lamellar-to-lamellar) centered at 43.7°C and a broad exothermic peak (lamellar-to-cubic phase) at 85.5°C. These two transitions are similar to those seen at pH 2.1 (Fig. 2, *bottom curve*), but with slightly different T_{tr} values (Table 2). Fig. 3 also shows that the high-temperature exothermic transition (at 85.5°C) in PLFE MLVs at pH 7.0 disappears in the second and third heating scan, similar to the trend obtained from PLFE MLVs at pH 2.1 (Fig. 1). The ΔH value for the lamellar-to-lamellar transition in PLFE MLVs at pH 7.0 (*Peak 1* in Fig. 3) is 10.0–16.0 kJ/mol (Table 3), which is comparable to the ΔH value (14.2 kJ/mol) (Table 2) for the lamellar-to-lamellar transition in PLFE MLVs at pH 2.1 (Fig. 2, *bottom curve* for Peak 1). Thus, a change in pH from 2.1 to 7.0 does not seem to have a great effect on DSC thermograms of PLFE MLVs.

The parameters associated with the endothermic lamellar-to-lamellar phase transition in all three scans in Fig. 3 are given in Table 3. The ΔH value of this phase transition is 10.0–16.0 kJ/mol (Table 3), which is ~2–3 times higher than that of the corresponding transition in PLFE MLVs derived from cells grown at 78°C (3.5–4.2 kJ/mol, Table 1). Again, the increase in ΔH with decreasing cell growth temperature can be explained by a decrease in the number of cyclopentane rings at a lower growth temperature, as discussed earlier. Taken together, it appears that the cell growth temperature (or, inferentially, the number of cyclopentane rings) is an important factor governing the thermodynamic properties of PLFE lipid membranes.

PPC scans measured at pH 2.1 for PLFE MLVs derived from cells grown at 78°C

PPC is a sensitive and accurate method to measure volumetric properties of biomolecules or bioassemblies and can yield useful information on their solvation in dilute solution. This relatively new technique has been applied to study proteins (21,36,37) and monopolar diester lipid membranes (38–40). In this study, we have used PPC to determine the relative volume change $\Delta V/V$ associated with the phase transitions mentioned above and the temperature dependence of the thermal expansion coefficient α for PLFE MLVs derived from different cell growth temperatures.

TABLE 3 DSC and PPC parameters of PLFE MLVs derived from cells grown at 65°C

DSC (pH 7.0)	Peak 1		
	T_{tr} (°C)	ΔH (kJ/mol)	$T_{1/2}$ (°C)
Scan 1	43.7	16.0	3.14
Scan 2	42.8	12.1	3.12
Scan 3	41.7	10.0	4.33
	Peak 1		
PPC	T_{tr} (°C)	$\Delta V/V$ (%)	$T_{1/2}$ (°C)
pH 7.0	43.0	0.56	4.0
pH 2.1	42.0	0.25	4.0

For the pH 7.0 and pH 2.1 measurements shown, the vesicles were dispersed in D_2O. Similar data were observed for the measurements in citrate buffer/H_2O solutions, except that the transition temperatures are shifted toward temperatures 2–3°C lower.

Fig. 4 shows the PPC results obtained from PLFE MLVs derived from cells grown at 78°C. The plot of the thermal volume expansion coefficient ($\alpha = (1/V)(\partial V/\partial T)_P$) (measured at pH 2.1) versus temperature (T) exhibits two small peaks, one centered at ~43–45°C and the other at 58–60°C. These transition temperatures coincide with the lamellar-to-lamellar phase transitions detected by DSC (Fig. 1) and small-angle x-ray scattering (22). In fact, the PPC measurements reveal a relative volume change ($\Delta V/V$, the area under the peak in the plot of α versus T) of 0.10–0.14% and 0.08–0.09% (Table 1) for those two transitions, shown in Fig. 4. These $\Delta V/V$ values are much smaller than the $\Delta V/V$ values of the main gel-to-fluid phase transition of saturated diacyl monopolar diester lipids, such as DMPC (2.8% (38)) and

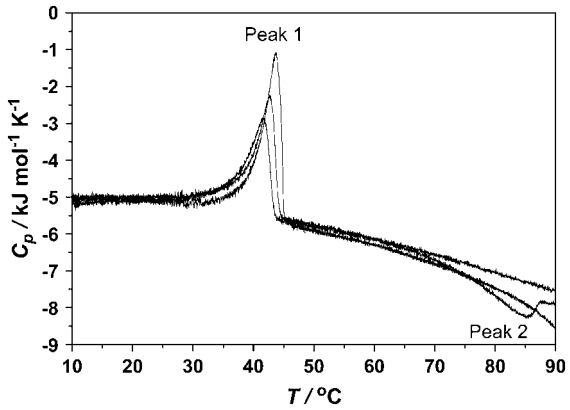

FIGURE 3 DSC profiles, measured at pH 7.0, of PLFE MLVs derived from cells grown at 65°C.

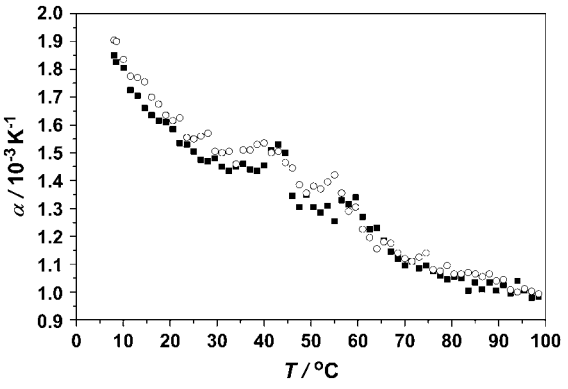

FIGURE 4 Plot of thermal expansion coefficient α versus temperature of PLFE MLVs at pH 2.1. PLFE was derived from cells grown at 78°C. Dark squares, Scan 1; open circles, Scan 2.

DPPC (~3%; see Fig. 6 and Table 4), and more comparable to the $\Delta V/V$ value (0.03–0.04%) of the pretransition in DPPC vesicles (Table 4) determined by the same PPC technique. The relatively low $\Delta V/V$ and small ΔH involved in the phase transitions help to explain why PLFE liposomes are remarkably thermally stable (discussed in Kanichay et al. (41)) and also echo the proposal that PLFE liposomes are generally rigid and tightly packed (7,9,11,13,15).

Unlike the first DSC heating thermogram (Fig. 1 and Fig. 2, *top curve*), the PPC scans do not reveal any significant peak in the 79–83°C region (Fig. 4). This result indicates that the high-temperature exothermic transition (lamellar-to-cubic phase) detected by DSC (Fig. 1 and Fig. 2, *top curve*) does not involve a significant volume change during the PPC run. Note that both DSC and PPC were run at the same effective scan rate (20°C/h).

PPC scans measured at pH 7.0 and 2.1 for PLFE MLVs derived from cells grown at 65°C

PPC measurements were also performed on PLFE MLVs derived from cells grown at a lower temperature, i.e., 65°C. A decrease in growth temperature should decrease the number of cyclopentane rings in the dibiphytanyl chain of PLFE lipids (6). It is then of interest to know how this structural change affects $\Delta V/V$ in PLFE liposomes. $\Delta V/V$ can originate from the volume change in the dibiphytanyl (hydrophobic) regions, from the polar headgroup regions where it has been suggested that an extensive hydrogen-bond network exists (16,17), or from both. In the polar headgroup regions, the changes in PLFE hydration could contribute to the change in the partial specific volume of PLFE.

For PLFE MLVs derived from cells grown at 65°C, the temperature dependence of α shows only one transition (~42–43°C) (Fig. 5) with $\Delta V/V$ values of 0.56% (measured at pH 7.0) and 0.25% (measured at pH 2.1) (Table 3). As mentioned earlier, the first heating DSC scan of this sample (Fig. 2, *bottom curve*, for measurement at pH 2.1, and Fig. 3 for measurement at pH 7.0) shows one endothermic peak centered at 43.7°C (pH 7.0) or at 51.0°C (pH 2.1) due to a lamellar-to-lamellar phase transition and a broad exothermic peak at 85.5°C (pH 7.0) or 83.2°C (pH 2.1) due to a lamellar-to-cubic phase transition. Thus, the PPC plot presented in Fig. 5 is consistent with the DSC data and shows once again that the lamellar-to-cubic phase transition detected at high temperatures (83.2–85.5°C) in the DSC thermograms (Figs. 2 and 3) does not involve any significant volume change. This is similar to the case for PLFE MLVs derived from cells grown at 78°C (Table 1 and Fig. 4). The $\Delta V/V$ value of the phase transition measured at pH 2.1 (0.25%) is ~2.1 times smaller than that measured at pH 7.0 (0.56%), suggesting that a decrease in pH from 7.0 to 2.1 tightens membrane packing. Another interesting point is that the $\Delta V/V$ value (0.56% at pH 7.0 and 0.25% at pH 2.1) for the lamellar-to-lamellar phase transition in PLFE MLVs derived from cells grown at 65°C is higher than that derived from cells grown at 78°C (0.08-0.14%). As our previous molecular modeling study (42) suggested, a decrease in the number of cyclopentane rings will make the PLFE membrane less tight and less rigid. Thus, it is reasonable that a higher $\Delta V/V$ is detected for the phase transition in PLFE MLVs derived from a lower growth temperature. A smaller $\Delta V/V$ for the phase transitions of lipid membranes derived from thermoacidophilic cells grown at a higher temperature

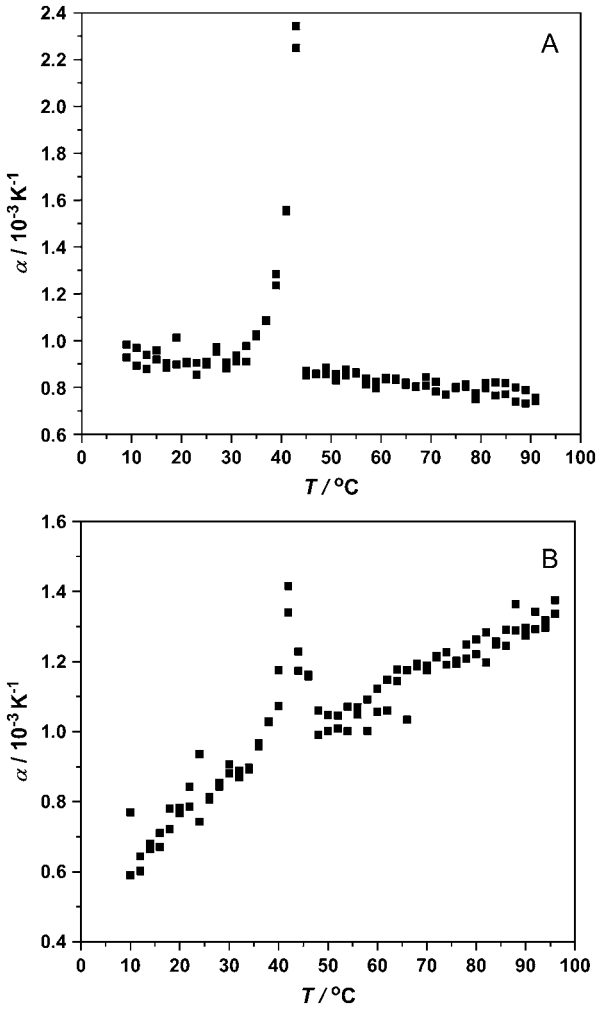

FIGURE 5 Plot of thermal expansion coefficient α versus temperature of PLFE liposomes at (*A*) pH 7.0 and (*B*) pH 2.1. PLFE was derived from cells grown at 65°C.

TABLE 4 PPC data of DPPC vesicles at pH 7.0

Peak 1			Peak 2		
T_{pre} (°C)	$\Delta V/V$ (%)	$T_{1/2}$ (°C)	T_m (°C)	$\Delta V/V$ (%)	$T_{1/2}$ (°C)
34.0	0.03–0.04	2.0	41.0	3.0 ± 0.3	1.98

Peak 1 corresponds to the pretransition (at T_{pre}), and Peak 2 to the main phase transition (at T_m).

explains why those cells can sustain a range of high growth temperatures without having membrane disruptions.

Temperature dependence of thermal expansion coefficient (α) in PLFE MLVs

In addition to $\Delta V/V$ through the phase transitions, PPC measurements provide information on the temperature dependence of the thermal expansion coefficient α. In PLFE MLVs derived from cells grown at 78°C (Fig. 4), the decrease of α with temperature is rather steep, changing from 1.80×10^{-3} K^{-1} at 10°C to 1.05×10^{-3} K^{-1} at 90°C. This marked decrease in α with increasing temperature could be due to the release of bound water from PLFE polar headgroups as is the case for proteins (36,37,43). For PLFE MLVs derived from cells grown at 65°C, the decrease of α (measured at pH 7.0) with temperature is much less steep (Fig. 5 *A*), changing from $\sim 0.95 \times 10^{-3}$ K^{-1} at 10°C to 0.75×10^{-3} K^{-1} at 90°C. In this case, the negative slope of α versus temperature can still be attributed to the release of some water from the polar headgroups. However, when measured at pH 2.1, PLFE MLVs derived from cells grown at 65°C exhibit an increase of α with increasing temperature (Fig. 5 *B*). The differences in the temperature dependence of α between Fig. 4 and Fig. 5 probably originate from the difference in cell growth temperature and the pH used for the experiments. It is known that a decrease in growth temperature of thermoacidophiles decreases the number of cyclopentane rings in tetraether lipids (6), which in turn affects the polar headgroup conformation (42). In a molecular modeling study, we have shown that, when the dibiphytanyl chains contain eight cyclopentane rings (the maximum number of cyclopentane rings in each dibiphytanyl chain), the polar headgroup of GDNT (the major component of PLFE) runs almost parallel to the membrane surface, but when the chains contain no rings, the polar headgroup is oriented perpendicular to the membrane surface (42). In the latter case, more lipid hydrophobic residues would be exposed to water, which could lead to a positive slope in the plot of α versus temperature, as is the case for hydrophobic hydration in proteins (36). It is also possible that the degree of hydration or the temperature dependence of polar headgroup dehydration in the PLFE polar headgroups varies with the headgroup conformation. These possibilities may explain why, at the same pH, the temperature dependence of α in PLFE MLVs varies with cell growth temperature (Fig. 4 versus Fig. 5 *B*). The effect of pH on the temperature dependence of α revealed in Fig. 5, *A* and *B*, may be due to changes in polar headgroup hydration and conformation as a result of changes in the degree of ionization on the phosphoinositol moiety of PLFE lipids. As the pH is changed from 2.1 (Fig. 5 *B*) to 7.0 (Fig. 5 *A*), the phosphoinositol group becomes more negatively charged, which would increase the hydration layer. Then, more water can be steadily released with increasing temperature, producing a negative slope in the plot of α versus temperature (Fig. 5 *A*).

It is interesting to note that whereas PLFE (a mixture of bipolar tetraether lipids) MLVs exhibit a negative slope in the plot of α versus temperature in some cases (Figs. 4 and 5 *A*), monopolar diester liposomes usually yield a positive slope. Using the same PPC technique, Heerklotz and Seelig (38) showed that α was 0.7×10^{-3} K^{-1} below the pretransition and 0.9×10^{-3} K^{-1} above the main transition for DMPC MLVs. A similar positive slope of α versus temperature in DMPC and DPPC vesicles was found in our study (Fig. 6) and in the PPC study by Wang and Epand (40). This positive slope was also found in unsaturated monopolar diester liposomes made of 1-palmitoyl-2-oleoyl-L-α-phosphatidylcholine and dioleoyl-L-α-phosphatidylcholine (38) and detected by non-PPC volumetric measurements on DMPC MLVs (44).

CONCLUDING REMARKS

In this study, we have used the combination of DSC and PPC to report, to our knowledge for the first time, the temperature-induced phase transitions and the associated ΔH and $\Delta V/V$ values as well as the temperature dependence of α in PLFE liposomes. The cell growth temperature dependence of ΔH and $\Delta V/V$ and the comparison with monopolar diester lipid vesicles shed new light on membrane packing in PLFE liposomes. Free volume and volume changes are important factors governing membrane properties such as solute partitioning and lateral diffusion. Based on this study and the previous works on PLFE liposomes, we can summarize membrane free volume or membrane volume changes of PLFE liposomes as follows (Fig. 7). First, in the temperature range 8–40°C, there is no phase transition detected by DSC (this study), PPC (this study), and small-angle x-ray scattering (22; also Fig. 7); however, there is formation of

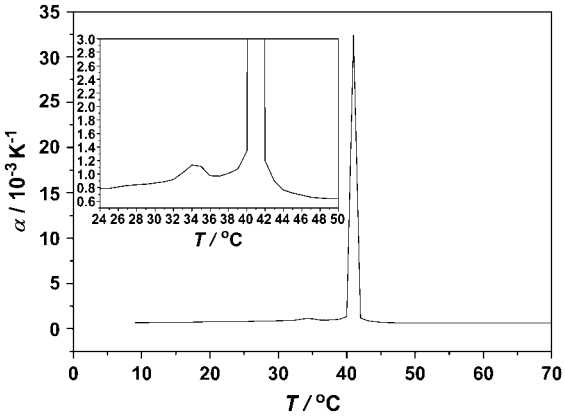

FIGURE 6 Plot of thermal expansion coefficient α versus temperature of DPPC vesicles (pH 7.0). (*Inset*) Expansion of the low-α data before and after the main transition temperature. Note that the DSC profile (not shown) of the same DPPC sample shows a pretransition at 34.8°C ($\Delta H = 8$ kJ/mol) and a main phase transition at 41.2°C ($\Delta H = 37$ kJ/mol).

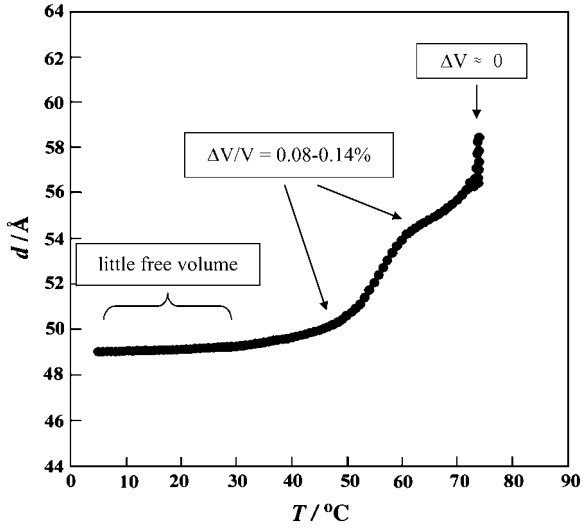

FIGURE 7 Summary of volumetric properties of PLFE liposomes at different temperature regions where either phase transitions are evident in the plot of the lamellar repeat unit (*d*-spacing, as revealed by small-angle x-ray scattering) versus temperature (copied from Chong et al. (22)) or microdomain formation occurs (7).

microdomains in the membrane at <20–24°C (7). Actually, below 20–24°C, there is little free volume in PLFE liposomes because those lipid microdomains were found to be laterally immobile in the plane of the membrane (7). Second, in the intermediate temperature region, two phase transitions can be detected at ~47–50°C and ~60°C by DSC (this study), PPC (this study), small-angle x-ray scattering (22; also Fig. 7), and fluorescent probes (7,15). These two transitions involve very small volume changes, with a $\Delta V/V$ equal to 0.08–0.14% (measured at pH 2.1, this study) in the case of PLFE MLVs derived from cells grown at 78°C. Third, at the high-temperature end, a lamellar-to-cubic phase transition was detected by DSC (this study) and small-angle x-ray scattering (22; also Fig. 7) at ~74–78°C, but there is no detectable volume change associated with this phase transition (this study). These volumetric properties of PLFE liposomes (summarized in Fig. 7) help us to understand why, despite the occurrence of thermal-induced phase transitions, PLFE liposomes exhibit an unusually low temperature sensitivity of proton permeation and dye leakage (9,10,11, 45,46) and a remarkable thermostability against autoclaving (P. Chong, V. English, D. Brown, and P. Cooke, unpublished results). Further, the observation that $\Delta V/V$ of PLFE MLVs becomes smaller when the cell growth temperature is increased from 65°C to 78°C and the pH is reduced from pH 7.0 to 2.1 agrees with the fact that thermoacidophilc archaea such as *S. acidocaldarius* thrive at high temperatures and acidic pH. Future DSC/PPC studies will employ the hydrolyzed PLFE (i.e., removing sugar and phosphate moieties) and quantify the number and distribution of cyclopentane rings in the PLFE dibiphytanyl chain to further understand the role of lipid structure in the thermodynamic properties of PLFE liposomes. This kind of physical characterization not only sheds light on how the plasma membrane of thermoacidophiles might sustain harsh growth conditions, but could also improve the use and design of archaeal bipolar tetraether (e.g., PLFE) liposomes in technological applications such as crystallization of membrane-bound proteins (47–50) and delivery of drugs, vaccines, and genes (51–54).

We are grateful for the Deutsche Forschungsgemeinschaft and the Fonds der Chemischen Industrie assistance (to R.W.) and the U.S. Army Research Office grant DAAD19-02-1-0077 (to P.L.-G.C.).

REFERENCES

1. Langworthy, T. A., and J. L. Pond. 1986. Membranes and lipids of thermophiles. *In* Thermophiles: General, Molecular, and Applied Microbiology. T. D. Brock, editor. John Wiley & Sons, New York. 107–134.
2. Kates, M. 1992. Archaebacterial lipids: structure, biosynthesis and function. *In* The Archaebacteria: Biochemistry and Biotechnology. M. J. Danson, D. W. Hough, and G. G. Lunt, editors. Portland Press, London. 51–72.
3. Lo, S.-L., and E. L. Chang. 1990. Purification and characterization of a liposomal-forming tetraether lipid fraction. *Biochem. Biophys. Res. Commun.* 167:238–243.
4. Sugai, A., R. Sakuma, I. Fukuda, N. Kurosawa, Y. H. Itoh, K. Kon, S. Ando, and T. Itoh. 1995. The structure of the core polyol of the ether lipids from *Sulfolobus acidocaldarius*. *Lipids.* 30:339–344.
5. Gliozzi, A., A. Relini, and P. L.-G. Chong. 2002. Structure and permeability properties of biomimetic membranes of bolaform archaeal tetraether lipids. *J. Membr. Sci.* 206:131–147.
6. De Rosa, M., E. Esposito, A. Gambacorta, B. Nicholaus, and J. D. Bu'lock. 1980. Effects of temperature on ether lipid composition of *Caldariella acidophila*. *Phytochemistry.* 19:827–831.
7. Bagatolli, L., E. Gratton, T. P. Khan, and P. L.-G. Chong. 2000. Two-photon fluorescence microscopy studies of bipolar tetraether giant liposomes from thermoacidophilic archaebacterial *Sulfolobus acidocaldarius*. *Biophys. J.* 79:416–425.
8. Elferink, M. G. L., J. G. de Wit, R. Demel, A. J. M. Driessen, and W. N. Konings. 1992. Functional reconstitution of membrane proteins in monolayer liposomes from bipolar lipids of *Sulfolobus acidocaldarius*. *J. Biol. Chem.* 267:1375–1381.
9. Chang, E. L. 1994. Unusual thermal stability of liposomes made from bipolar tetraether lipids. *Biochem. Biophys. Res. Commun.* 202: 673–679.
10. Elferink, M. G. L., J. G. de Wit, A. J. M. Driessen, and W. N. Konings. 1994. Stability and proton-permeability of liposomes composed of archaeal tetraether lipids. *Biochim. Biophys. Acta.* 1193:247–254.
11. Komatsu, H., and P. L.-G. Chong. 1998. Low permeability of liposomal membranes composed of bipolar tetraether lipids from thermoacidophilic archaebacterium *Sulfolobus acidocaldarius*. *Biochemistry.* 37:107–115.
12. Baba, T., H. Minamikawa, H. Masakatsu, and T. Handa. 2001. Hydration and molecular motions in synthetic phytanyl-chained glycolipid vesicle membranes. *Biophys. J.* 81:3377–3386.
13. Kao, Y. L., E. L. Chang, and P. L.-G. Chong. 1992. Unusual pressure dependence of the lateral motions of pyrene-labeled phosphatidylcholine in bipolar lipid vesicles. *Biochem. Biophys. Res. Commun.* 188: 1241–1246.
14. Jarrel, H. C., K. A. Zukotynski, and G. D. Sprott. 1998. Lateral diffusion of the total polar lipids from *Theroplasma acidophilum* in multilamellar liposomes. *Biochim. Biophys. Acta.* 1369:259–266.
15. Khan, T. K., and P. L.-G. Chong. 2000. Studies of archaebacterial bipolar tetraether liposomes by perylene fluorescence. *Biophys. J.* 78: 1390–1399.

16. Elferink, M. G. L., J. G. de Wit, A. J. M. Driessen, and W. N. Konings. 1993. Energy-transducing properties of primary proton pumps reconstituted into archaeal bipolar lipid vesicles. *Eur. J. Biochem.* 214:917–925.

17. Vilalta, I., A. Gliozzi, and M. Prats. 1996. Interfacial air/water proton conduction from long distances by *Sulfolobus solfataricus* archaeal bolaform lipids. *Eur. J. Biochem.* 240:181–185.

18. Bruno, S., S. Cannistraro, A. Gliozzi, M. De Rosa, and A. Gambacorta. 1985. A spin label ESR and saturation transfer-ESR study of archaebacteria bipolar lipids. *Eur. Biophys. J.* 13:67–76.

19. Chang, E. L., and S.-L. Lo. 1991. Extraction and purification of tetraether lipids from *Sulfolobus acidocaldarius*. *In* Protocols for Archaebacterial Research. E. M. Fleischmann, A. R. Place, R. T. Robb, and H. J. Schreier, editors. Maryland Biotechnology Institute, University of Maryland System, Baltimore. 2.3.1–2.3.14.

20. Dzwolak, W., R. Ravindra, J. Lendermann, and R. Winter. 2003. Aggregation of bovine insulin probed by DSC/PPC calorimetry and FTIR spectroscopy. *Biochemistry.* 42:11347–11355.

21. Ravindra, R., and R. Winter. 2004. Pressure perturbation calorimetry: a new technique provides surprising results on the effects of cosolvents on protein solvation and unfolding behaviour. *ChemPhysChem.* 5:566–571.

22. Chong, P. L.-G., M. Zein, T. K. Khan, and R. Winter. 2003. Structure and conformation of bipolar tetraether lipid membranes derived from thermoacidophilic archaeon *Sulfolobus acidocaldarius* as revealed by small-angle x-ray scattering and high pressure FT-IR spectroscopy. *J. Phys. Chem.* 107:8694–8700.

23. Slater, J. L., and C. Huang. 1987. Scanning calorimetry reveals a new phase transition in L-α-dipalmitoylphosphatidylcholine. *Biophys. J.* 52:667–670.

24. Tenchov, B., R. Koynova, and G. Rapp. 2001. New ordered metastable phases between the gel and subgel phases in hydrated phospholipids. *Biophys. J.* 80:1873–1890.

25. Siegel, D. P. 1986. Inverted micellar intermediates and the transitions between lamellar, cubic, and inverted hexagonal amphiphile phases. III. Isotropic and inverted cubic state formation via intermediates in transitions between L_α and H_{II} phases. *Chem. Phys. Lipids.* 42:279–301.

26. Siegel, D. P., and J. L. Banschbach. 1990. Lamellar/inverted cubic (L_α/Q_{II}) phase transition in N-methylated dioleoylphosphatidylethanolamine. *Biochemistry.* 29:5975–5981.

27. Czeslik, C., R. Winter, G. Rapp, and K. Bartels. 1995. Temperature- and pressure-dependent phase behavior of monoacylglycerides monoolein and monoelaidin. *Biophys. J.* 68:1423–1429.

28. Gulik, A., V. Luzzati, M. de Rosa, and A. Gambacorta. 1985. Structure and polymorphism of bipolar isopranyl ether lipids from archaebacteria. *J. Mol. Biol.* 182:131–149.

29. Luzzati, V., A. Gulik, M. DeRosa, and A. Gambacorta. 1987. Lipids from *Sulfolobus solfataricus*, life at high temperature and the structure of membranes. *Chem. Scr.* 27B:211–219.

30. Gulik, A., V. Luzzati, M. de Rosa, and A. Gambacorta. 1988. Tetraether lipid components from a thermoacidophilic archaebacterium. *J. Mol. Biol.* 201:429–435.

31. Koynova, R., and M. Caffrey. 1998. Phase and phase transitions of the phosphatidylcholines. *Biochim. Biophys. Acta.* 1376:91–145.

32. Mabrey, S., and J. M. Sturtevant. 1976. Investigation of phase transitions of lipids and lipid mixtures by high sensitivity differential scanning calorimetry. *Proc. Natl. Acad. Sci. USA.* 73:3862–3866.

33. Janiak, M., D. M. Small, and G. G. Shipley. 1976. Nature of the thermal pretransition of synthetic phospholipids: dimyristoyl- and dipalmitoyllecithin. *Biochemistry.* 15:4575–4580.

34. Sugar, I. P., E. Michonova-Alexova, and P. L.-G. Chong. 2001. Geometrical properties of gel and fluid clusters in DMPC/DSPC bilayers: Monte Carlo simulation approach using a two-state model. *Biophys. J.* 81:2425–2441.

35. Cherezov, V., D. P. Siegel, W. Shaw, S. W. Burgess, and M. Caffrey. 2003. The kinetics of non-lamellar phase formation in DOPE-Me: relevance to biomembrane fusion. *J. Membr. Biol.* 195:165–182.

36. Lin, L.-N., J. F. Brandts, J. M. Brandts, and V. Plotnikov. 2002. Determination of the volumetric properties of proteins and other solutes using pressure perturbation calorimetry. *Anal. Biochem.* 302: 144–160.

37. Cordeiro, Y., J. Kraineva, R. Ravindra, L. M. T. R. Lima, M. P. B. Gomes, D. Foguel, R. Winter, and J. L. Silva. 2004. Hydration and packing effects on prion folding and β-sheet conversion: High-pressure spectroscopy and pressure perturbation calorimetry studies. *J. Biol. Chem.* 279:32354–32359.

38. Heerklotz, H., and J. Seelig. 2002. Application of pressure perturbation calorimetry to lipid bilayers. *Biophys. J.* 82:1445–1452.

39. Grabitz, P., V. P. Ivanova, and T. Heimburg. 2002. Relaxation kinetics of lipid membranes and its relation to the heat capacity. *Biophys. J.* 82:299–309.

40. Wang, S.-L., and R. M. Epand. 2004. Factors determining pressure perturbation calorimetry measurements: evidence for the formation of metastable states at lipid phase transitions. *Chem. Phys. Lipids.* 129: 21–30.

41. Kanichay, R., L. T. Boni, P. H. Cooke, T. K. Khan, and P. L.-G. Chong. 2003. Calcium-induced aggregation of archaeal bipolar tetraether liposomes derived from thermoacidophilic archaeon *Sulfolobus acidocaldarius*. *Archaea.* 1:175–183.

42. Gabriel, J. L., and P. L.-G. Chong. 2000. Molecular modeling of archaebacterial bipolar tetraether lipid membranes. *Chem. Phys. Lipids.* 105:193–200.

43. Ravindra, R., and R. Winter. 2003. Pressure perturbation calorimetric studies of the solvation properties and the thermal unfolding of proteins in solution. *Z. Phys. Chem.* 217:1221–1243.

44. Bottner, M., and R. Winter. 1993. Influence of the local anesthetic tetracaine on the phase behavior and the thermodynamic properties of phospholipid bilayers. *Biophys. J.* 65:2041–2046.

45. In't Veld, G., M. G. L. Elferink, A. J. M. Driessen, and W. N. Konings. 1992. Reconstitution of the leucine transport system of *Lactococcus lactis* into liposomes composed of membrane-spanning lipids from *Sulfolobus acidocaldarius*. *Biochemistry.* 31:12493–12499.

46. Van de Vossenberg, J. L. C. M., T. Ubbink-Kok, M. G. L. Elferink, A. J. M. Driessen, and W. N. Konings. 1995. Ion permeability of the cytoplasmic membrane limits the maximum growth temperature of bacteria and archaea. *Mol. Microbiol.* 18:925–932.

47. Landau, E. M., and J. P. Rosenbusch. 1996. Lipidic cubic phases: a novel concept for the crystallization of membrane proteins. *Proc. Natl. Acad. Sci. USA.* 93:14532–14535.

48. Pebay-Peyroula, E., G. Rummel, J. P. Rosenbusch, and E. M. Landau. 1997. X-ray structure of bacteriorhodopsin at 2.5 Å from microcrystals grown in lipidic cubic phases. *Science.* 277:1676–1681.

49. Gouaux, E. 1998. It's not just a phase: crystallization and X-ray structure determination of bacteriorhodopsin in lipidic cubic phases. *Structure.* 6:5–10.

50. Chiu, M. L., P. Nollert, M. C. Loewen, H. Belrhali, E. Pebay-Peyroula, J. P. Rosenbusch, and E. M. Landau. 2000. Crystallization in cubo: general applicability to membrane proteins. *Acta Crystallogr. D Biol. Crystallogr.* 56:781–784.

51. Tomioka, K., F. Kii, H. Fukuda, and S. Katoh. 1994. Homogeneous immunoassay of antibody by use of liposomes made of a model lipid of archaebacteria. *J. Immunol. Methods.* 176:1–7.

52. Freisleben, H.-J., J. Bormann, D. C. Litzinger, F. Lehr, P. Rudolph, M. Schatton, and L. Huang. 1995. Toxicity and biodistribution of liposomes of the main phospholipid from the archaebacterium *Thermoplasma acidophilum*. *J. Liposome Res.* 5:215–223.

53. Gliozzi, A., and A. Relini. 1996. Lipid vesicles as model systems for archaea membranes. *In* Handbook of Nonmedical Applications of Liposomes, Vol. II. Y. Barenholz, and D. D. Lasic, editors. CRC Press, Boca Raton, FL. 329–348.

54. Krishnan, L., C. J. Dicaire, G. B. Patel, and G. D. Sprott. 2000. Archaeosome vaccine adjuvants induce strong humoral, cell-mediated, and memory responses: comparison to conventional liposomes and alum. *Infect. Immun.* 68:54–63.